Title	Barnacle Cement Proteins-Inspired Tough Hydrogels with Robust, Long-Lasting, and Repeatable Underwater Adhesion
Author(s)	Fan, Hailong; Wang, Jiahui; Gong, Jian Ping
Citation	Advanced Functional Materials, 31(11), 2009334 https://doi.org/10.1002/adfm.202009334
Issue Date	2020-12-28
Doc URL	https://hdl.handle.net/2115/83723
Rights	This is the peer reviewed version of the following article: Fan, H., Wang, J., Gong, J. P., Barnacle Cement Proteins-Inspired Tough Hydrogels with Robust, Long-Lasting, and Repeatable Underwater Adhesion. Adv. Funct. Mater. 2021, 31, 2009334., which has been published in final form at https://doi.org/10.1002/adfm.202009334. This article may be used for non-commercial purposes in accordance with Wiley Terms and Conditions for Use of Self-Archived Versions.
Type	journal article
File Information	an-adv func mater.pdf

Barnacle Cement Proteins Inspired Tough Hydrogels with Robust, Long-lasting, and Repeatable Underwater Adhesion

Hailong Fan, Jiahui Wang, and Jian Ping Gong*

Dr. H. L. Fan, Prof. J. P. Gong
Institute for Chemical Reaction Design and Discovery (WPI-ICReDD), Hokkaido University, N21W10, Kita-ku, Sapporo 001-0021, Japan
E-mail: gong@sci.hokudai.ac.jp

J. H. Wang
Graduate School of Life Science, Hokkaido University, N21W11, Kita-ku, Sapporo 001-0021, Japan

Prof. J. P. Gong
Faculty of Advanced Life Science, Hokkaido University, N21W11, Kita-ku, Sapporo 001-0021, Japan
Global Station for Soft Matter GI-CoRE, Hokkaido University, N21W11, Kita-ku, Sapporo 001-0021, Japan

The development of adhesives that can achieve robust and repeatable adhesion to various surfaces underwater is promising; however, this remains a major challenge primarily because the surface hydration layer weakens the interfacial molecular interactions. Herein, we propose a strategy to develop tough hydrogels that are robust, reusable, and long-lasting for underwater adhesion. We synthesized hydrogels from cationic and aromatic monomers with an aromatic-rich composition inspired by the amino acid residuals in barnacle cement proteins. The hydrogels are mechanically strong and tough (elastic modulus 0.35 MPa, fracture stress 1.0 MPa, and fracture strain 720%), owing to the interchain π-π and cation-π interactions. In water, the hydrogels firmly adhere to diverse surfaces through interfacial electrostatic and hydrophobic interactions (adhesion strength of 180 kPa), which allows for instant adhesion and reversibility (50 times). Moreover, the hydrogel shows long-lasting adhesion in water for months (100 days). Novel adhesive hydrogels may be useful in many applications, including underwater transfer, water-based devices, underwater repair, and underwater soft robots.

1. Introduction

Underwater adhesives, both permanent or reusable, are required in many applications, including underwater repair, transfer printing, implantable devices, wound dressing, and water-based energy devices.[1] Recently, significant progress has been made in the design and fabrication of underwater adhesives using diverse strategies, which can be roughly classified into two categories: glue-type and tape-type adhesives. The former are liquid solutions (e.g., coacervates,[2] polymer solutions,[3] liquid polymers,[4] and monomer solutions[5]) that require a curing process to achieve interfacial bonding in water. The latter are solid materials (e.g., polymer films,[6] rubbers,[7] and hydrogels[8]) that can directly adhere to the substrates underwater. The bonding strengths of glue-type adhesives are usually robust (> 100 kPa) but require long curing times (hours to days) and they cannot be reused. In contrast, tape-like adhesives are instant and reusable. Among tape-type adhesives, biostructure-inspired underwater adhesives, which are based on the suction effect accompanied by capillarity, typically exhibit outstanding adhesion performance; however, they require delicate structural design and complicated fabrication processes.[9] For tape-like adhesives that are completely based on molecular interaction, the adhesion strengths are usually weak (< 50 kPa).[8a, 10] This is due to the non-covalent interaction at the interface being significantly weakened by the hydration layer from the water. This is especially true for hydrogels, where it is harder to achieve strong underwater adhesion due to their polymer hydrophilicity and highly swelled network as compared to those of the rubber adhesives. In addition, ideal underwater adhesives also require long-lasting adhesion stability in water, which has seldom been studied.[8a, 8f] Therefore, developing adhesives that exhibit robust, instant, repeatable, and long-lasting adhesion in water is still a challenge in adhesion science and engineering.

Generally, a repeatable and robust adhesion requires both a strong non-covalent interaction at the interface and a high toughness of the bulk material, as illustrated in **Figure 1**a.[8f, 11] To be considered a good adhesive, the material is required to be highly stretchable with large

fracture stress (σ_c), fracture strain (ε_c), and the interfacial bonding strength (σ_a) being greater than the yielding stress (σ_y) to ensure that the material can undergo considerable deformation to dissipate a large amount of energy during the debonding process. To apply this principle to hydrogel adhesives, the hydrogels need to remain stretchable and tough at the swelling equilibrium state in water, without showing cohesive failure during debonding. Additionally, the hydrogels are required to have the ability to break the hydration layer and form strong physical interactions with the surface of substrates (high σ_a). A molecular design principle for tough hydrogels is incorporating reversible dynamic bonds that can dissipate energy during deformation.[12] Such design principles have been proven effective for many non-covalent bonds, including ionic bonds, hydrogen bonds, and hydrophobic interactions. In contrast, the molecular design principle for attaining strong non-covalent interfacial bonding in water is much less understood. It was found that the catechol group inspired by mussel foot proteins can form strong interactions with diverse substrates under acidic conditions, but it is easily oxidized to lose adhesion under realistic conditions.[13] Many solid surfaces, including rocks, glass, and metal, are negatively charged in an aqueous environment.[14] Thus, electrostatic interaction could be utilized as a major alternative mechanism for adhesives that are applied to these surfaces. However, hydrogels containing ionic groups, referred to as polyelectrolyte gels, swell significantly in water due to the high ionic osmotic pressure of dissociated counterions. Consequently, polyelectrolyte hydrogels are fragile and mechanically weak in water. Although tough hydrogels and strong adhesion polymers have been developed, combining them in one hydrogel is still challenging.

Investigating marine sessile organisms is an efficient way to develop underwater adhesives. For example, mussels and tubeworms are the star organisms from a scientific perspective because their specific post-translationally modified amino acids (3,4-dihydroxyphenyl-L-alanine (DOPA) and phosphorylated serine) play important roles in their underwater adhesion

mechanisms.[15] In comparison, limited attention has been paid to barnacles because their cement proteins (CPs) only consist of common amino acids (Figure 1b).[16] Advances in the study of barnacles have revealed an entirely different molecular adhesion mechanism. It was found that the concentrations of cationic Arg and Lys and those of aromatic Phe and Tyr are relatively high in bulk CPs (CP52K and CP100K), which enhances the cohesion strength by forming strong hydrophobic interactions and cation-π interactions.[17] The CPs found at the interface (CP19K and CP68K) contain high amounts of cationic Lys and hydrophobic amino acids.[18] It has been speculated that, with the cooperative role of neighboring hydrophobic amino acids, cationic Lys forms strong electrostatic interactions with the negatively charged rock surface.[19] Although the adhesion mechanism of the barnacle has not been fully uncovered, these specificities of CPs may allow a new conceptual design for underwater adhesives.

2. Results and Discussion

Inspired by barnacle CPs, we developed a tough hydrogel that exhibits repeatable and robust underwater adhesion to various substrates. The hydrogel consists of a cross-linked copolymer of cationic 2-(acryloyloxy)ethyl trimethylammonium chloride (ATAC) and aromatic 2-phenoxyethyl acrylate (PEA) monomers, which mimic the cationic and hydrophobic amino acids in CPs, respectively (Figure 1c). The hydrogel was obtained by a simple free-radical copolymerization of monomers in the presence of a small amount of a chemical cross-linker in the dimethyl sulfoxide (DMSO) solution, which was followed by swelling in water (Table S1, Supplementary Information). In the bulk hydrogel, the strong π-π and cation-π interactions function as dynamic cross-links to enhance the toughness and cohesion strength (high σ_c). The aromatic groups can break the hydration layer on the surfaces, thereby providing an interior region with a low dielectric constant to enhance the electrostatic interactions of neighboring cationic groups; further, they can also form interfacial

hydrophobic bonds.[20] Consequently, the hydrogel achieves robust and reversible underwater adhesion (high debonding stress σ_a).

Achieving a high-performance hydrogel requires balancing the hydrophobic/cation-π attraction and electrostatic repulsion between polymer chains because strong interchain attraction leads to deswelling and high stiffness of the hydrogel, while strong interchain repulsion by the osmotic pressure of the dissociated counterions leads to swelling and fragileness of the hydrogel, both resulting in poor adhesion. In this study, a series of poly(ATAC-co-PEA) hydrogels with various hydrophobic monomer molar fractions (f) were fabricated. For f = 0.7, the gel highly swelled in water, indicating that the strong osmotic repulsion prevents the aggregation of hydrophobic groups and interchain cation-π interactions. As a result, the hydrogel shows purely elastic properties (Figure S1a, Supplementary Information) and weak mechanical strength. Increasing the PEA fraction weakens the osmotic repulsion of polymer chains but strengthens the π-π and cation-π attraction. As a result, the water content and the swelling ratio of the hydrogel decreased dramatically with an increase in f (**Figure 2**a), and the hydrogel changed from transparent to translucent, indicating the formation of large aggregates (Figure 2b). Moreover, the surface of the hydrogel became more hydrophobic, as shown by the change in the contact angle with water from 67.3 to 85.4° (Figure 2b). However, further increasing the PEA fraction (f = 0.9) led to an extremely strong attraction between the polymer chains; consequently, the hydrogel significantly shrank, showing an irregular shape with an inhomogeneous structure.[21]

Given the dynamic nature of the π-π and cation-π interactions, the hydrogels with high PEA fractions (f = 0.8 and 0.85) are strongly viscoelastic (Figure S1b and S1c, Supplementary Information) and mechanically tough. For example, a string of f = 0.85 gel with a 2 mm^2 cross-section can sustain a weight of 0.1 kg (Figure 2c). Figure 2d shows the tensile stress-strain curves of the hydrogels. Compared with the f = 0.7 gel, which is

mechanically weak and fragile, the f = 0.8 and 0.85 gels have significantly enhanced

cohesion. For instance, the tensile strength of the f = 0.85 hydrogel was approximately 1.0

MPa with an elongation of 750% and the elastic modulus was approximately 0.35 MPa

(Figure S2 and Table S2, Supplementary Information). It also had a clear yielding at a stress

of approximately 0.12 MPa. Moreover, as revealed by the Mooney–Rivlin plot,[22] the highly

swollen f = 0.7 gel showed distinct strain hardening during the deformation, while tough gels

of f = 0.8 and 0.85 showed strain softening and then strain hardening, indicating a large

number of dynamic bonds acting as cross-linkers in the networks (Figure S3, Supplementary

Information). Successive loading-unloading tests were performed to investigate the energy

dissipation process of the f = 0.85 gel (Figure 2e). The area between the loading and

unloading curves indicates the effective energy dissipation, and the dissipation area increases

with the stretch strain (Figure S4, Supplementary Information). Moreover, the overlap

between two successive cycles indicates a fast self-recovering ability of the hydrogel. For

example, at a strain of 200%, the sample showed approximately 100% recovery in the second

loading after a 2 min wait (Figure 2f). The self-recoverable, dissipative matrix satisfies one of

the two requirements for tough adhesion.

We tested the adhesiveness of poly(ATAC-co-PEA) hydrogels in water using a tack test

(**Figure 3**a). The highly swollen f = 0.7 hydrogel adhered to the glass substrate firmly, and the

detachment occurred at the bulk of the gel, namely cohesion failure, due to its fragile

mechanical property (Figure 3b). For hydrogels with high PEA fractions (f = 0.8 and 0.85),

the adhesions to the glass surface in water were firm, and the gels underwent a considerable

deformation to dissipate a large amount of energy during the retracting process before joint

failure. For example, the f = 0.85 hydrogel with a water content of 62 wt% exhibited strong

adhesiveness. The adhesive strength approached 180 kPa, which was higher than its yielding

stress (120 kPa) to show adhesion energy of approximately 70 J m^{-2}. Figure 3d demonstrates

that the f = 0.85 hydrogel with a 15 mm diameter and 1.0 mm thickness can rapidly adhere

and lift a 1.2 kg submerged block out of the water without failure of the adhesion (Movie 1, Supplementary Information). Figure 3e shows that the f = 0.85 hydrogel can mend a hole in a plastic bag and immediately stop the water leakage (Movie 2, Supplementary Information).

Owing to the fast formation of non-covalent interactions at the interface, the adhesion of the hydrogels in water is rapid and reversible. The repeat adhesion test showed that the f = 0.85 hydrogel maintained its robust underwater adhesion even after 50 adhesion-detachment cycles (Figure 3f). This repeatable adhesion allows for the poly(ATAC-co-PEA) hydrogels to be used in a broad range of practical applications, such as reversible material transfer, temporary fixation, and material separation. In addition, the adhesion of the f = 0.85 hydrogels in water has long-lasting stability, measured by lap shear test. Their underwater adhesion strength did not decrease after 100 days (Figure 3g). Figure 3h shows that the f = 0.85 hydrogel has strong underwater adhesion to the glass slides and can successfully hold a weight of 1.0 kg in water after 60 days.

The adhesion of poly(ATAC-co-PEA) hydrogels to diverse substrates was further tested (Figure 3i). The results indicated that the hydrogels have strong adhesion to negatively charged, hydrophobic, and metal surfaces. To our surprise, the hydrogels also showed good adhesion to a positively charged glass (-NH_4^+ functionalized), indicating that hydrophobic interactions, hydrogen bonds, and cation-π interactions also play roles in adhesion. Among them, the adhesion to the negatively charged surface was the strongest, confirming that the electrostatic interaction contributes the most to the high adhesion strength.

The adhesion of poly(ATAC-co-PEA) adhesive hydrogels in different solutions was also tested. The f = 0.85 hydrogel exhibited the same excellent adhesion as that in water in a wide range of pH solutions from pH 4 to pH 10, (Figure S5, Supplementary Information). However, in a solution with very high ionic strength, the hydrogels deswelled and the underwater adhesion changed dramatically. At 0.7 M NaCl solution (ionic strength of seawater), the electrostatic repulsion of polymer chains is screened, leading to the volume

shrinkage of hydrogels (Table S2, Supplementary Information). The tensile-test showed that

the mechanical properties of poly(ATAC-co-PEA) hydrogels in saline water improved

significantly (Figure S6, Supplementary Information). To better understand the effect of

volume change on the mechanical properties, we normalized the tensile stress-strain curves of

hydrogels by the swelling ratio (Q) (Figure S7, Supplementary Information). Compared with

poly(ATAC-co-PEA) gels in water, the normalized elastic modulus and stress of gels in 0.7 M

NaCl is lower but the gels are more extensible, which may indicate that the screen effect of

salt ions only caused the shrink of pre-stretched chains but did not enhance the hydrophobic

interaction significantly. Due to the change of mechanical properties of hydrogels in salt

solution, the underwater adhesion abilities of hydrogels also changed (Figure S8,

Supplementary Information). For $f = 0.7$ hydrogel, the underwater adhesion dramatically

increased due to the enhanced cohesive strength. In contrast, for hydrogels with high PEA

fractions ($f = 0.8$ and 0.85), the underwater adhesion decreased significantly because of their

high stiffness.

   To determine the importance of cationic and aromatic groups in high-performance

hydrogels, we fabricated control hydrogels with different monomer pairs. We first changed

the aromatic PEA monomer to a hydrophobic epoxy monomer (5-ethyl-1,3-dioxan-5-yl)

methyl acrylate (EDMA) and fabricated hydrogels from the cationic/epoxy pair. Next, we

changed the cationic ATAC monomer to an anionic 3-sulfopropyl acrylate potassium (SPAK)

monomer and fabricated hydrogels from the anionic/aromatic pair, respectively (**Figure 4**a).

In the equilibrium state, the control hydrogels were highly swollen compared with

poly(ATAC-co-PEA) gels of the same hydrophobic monomer fraction, particularly for the

poly(ATAC-co-EDMA) gels with no aromatic monomer (Table S1, Supplementary

Information). The tensile stress–strain curves of the hydrogels show that the mechanical

strength of the control hydrogels is relatively weak, particularly for $f = 0.8$ (Figure 4b). A

further increase in the hydrophobic monomer ratio of the control hydrogels ($f = 0.85$) can

enhance their mechanical strength; however, they are still much weaker than the poly(ATAC-co-PEA) gel of f = 0.85 (Figure 4c). Considering the differences in the swelling ratio of hydrogels, we compared the tensile stress-strain curves of hydrogels normalized by the swelling ratio (Q) (Figure S9, Supplementary Information). It was found that the normalized mechanical strength of poly(ATAC-co-PEA) gel is still much stronger than that of the control hydrogels, which indicates that cation-π interactions play an important role in its tough cohesion. The adhesiveness of the control hydrogels was also tested. The adhesion on the negatively charged surface of hydrogels with cationic/epoxy pairs is weak because of their high swelling ratio (Figure 4d). Hydrogels with anionic/aromatic pairs showed relatively strong underwater adhesion to a positively charged surface, but weak adhesion to the other types of substrates (Figure 4e and 4f). These results indicate that both cationic and aromatic groups play important roles in the cohesion and adhesion of poly(ATAC-co-PEA) hydrogels, due to the strong π-π and cation-π interactions. Moreover, the robust adhesion between hydrogels and charged surfaces implies that, with the aid of neighboring aromatic groups that break the hydration layer, the electrostatic interactions can provide robust interfacial adhesion in water.

Finally, we compared the underwater adhesion strength (σ_a) and cohesion strength (σ_c) of various hydrogels (**Figure 5** and Table S3, Supplementary Information). Compared with other types of adhesives that exhibit rapid underwater molecular bonding reported in literatures, the poly(ATAC-co-PEA) (f = 0.85) hydrogels developed in this work, shortly named as P(cation-π_{rich}) gel, show superior adhesion strength, along with a high modulus and cohesion strength.

3. Conclusions

In summary, novel underwater adhesive hydrogels inspired by barnacle CPs were developed. The hydrogels, made from copolymerization of cationic and aromatic monomers with an aromatic-rich composition, showed not only excellent mechanical strength and

toughness but also robust, repeatable, and long-lasting underwater adhesion to diverse substrates. In these hydrogel networks, the π-π and cation-π interactions provide many physical cross-linkers that increase mechanical cohesion and energy dissipation. At the interface, the aromatic groups play dual roles, providing hydrophobic adhesion and enhancing the electrostatic adhesion of their neighboring cationic groups. This work also provides insight on the role of cationic and aromatic amino acids in barnacle CPs.

4. Experimental Section

Materials: 2-(acryloyloxy)ethyl trimethyl ammonium chloride (ATAC, 79.4% in water), 2-phenoxyethyl acrylate (PEA), and (5-Ethyl-1,3-dioxan-5-yl) methyl acrylate (EDMA) were provided by Osaka Organic Chemical Co., Ltd., Japan. 3-sulfopropyl acrylate potassium (SPAK), N,N'-methylenebis(acrylamide) (MBAA), 2-oxoglutaric acid, NaCl, and dimethyl sulfoxide (DMSO) were purchased from Wako Pure Chemical Industries, Ltd. All of the chemicals were used as purchased without further purification. Millipore deionized water was used in all of the experiments.

Hydrogel synthesis: The formulation of hydrogels is shown in Table S1. All hydrogels were synthesized using the one-step random copolymerization of the prescribed monomers in DMSO. The monomers (total monomer concentration 2.4 M) with prescribed hydrophobic monomer molar fraction f, UV initiator (2-oxoglutaric acid, 6 mM) and chemical crosslinker (MBAA, 2.4 mM) were first dissolved in DMSO, and then the resulting mixture was poured into a reaction cell consisting of a pair of glass plates with a 1-mm spacing and irradiated at 365 nm UV with intensity of 4 mW cm^{-2} for 11 h in glovebox. After the polymerization, the as-prepared gel was immersed in a large amount of water to wash away the DMSO and residual chemicals. The water was exchanged every 12 h for over 1 week, after that the samples reached equilibrium. Before the test, the hydrogels were stored in water. The water content of hydrogels was measured using Moisture Balance (SHIMADZU, MOC-120H).

Mechanical test: The tensile stress–strain measurements were performed using a universal testing machine (UTM, INSTRON 5965) at a steady velocity of 100 mm min^{-1} in air. The samples were cut into a dumbbell-shape with the standard JIS-K6251-7 size (12 mm (L) × 2 mm (d) × 1~2 mm (w)). The elastic modulus (E) was calculated from the slope over 4–8% of the strain of the stress–strain curve. The tensile stress was calculated from the tensile force divided by the cross-section area of the virgin sample. The tensile strain was calculated from the displacement of the cross-head of the testing machine divided by the initial gauge length (12 mm). The initial strain rate was calculated from the deformation velocity divided by the initial gauge length.

Rheological test: Rheological tests were performed using an ARES-G2 rheometer (TA Instruments). A rheological angular frequency sweep from 0.01 to 100 rad s^{-1} was performed with a shear strain of 0.1% in the parallel-plate geometry at 24°C. The disc-shaped samples with thicknesses of approximately 1.5 mm and diameters of 15 mm were placed on the plates and surrounded by water.

Adhesion test: The tack test was used to characterize the adhesiveness. The substrates used were commercially available glass (Matsunami Glass, Osaka, Japan, S2112), positively charged glass (MAS-coated Superfrost, Matsunami Glass, Osaka, Japan, S9441), poly(propene) (PP), polymethyl methacrylate (PMMA), polycarbonate (PC), stainless steel (SS), and Aluminum (Al). The substrates were rinsed with ethanol, and then with deionized water before use. The test was performed on the SHIMADZU tester (autograph AG-X) with Trapezium X software. To perform the experiment, the hydrogel with a diameter of 15 mm and thickness of approximately 1.2–2.0 mm was first glued to the probe using cyanoacrylate (super glue), and then the gel (on the probe) was immersed into the test solution for 5 min so that it can reach equilibrium before the test. The probe approached the substrate surface at a speed of 10 μm s^{-1}, held by the applied pressure for 10 s, and then retracted at a rate of 100

μm s^{-1}. To insure the full contact between tough hydrogel and substrate, a pressure equals to the elastic modulus of the tested sample was applied in the tack test.

All the tests were performed underwater at room temperature. For the long-lasting adhesion in water, the lap shear test has been used. A disc shape hydrogel (diameter 15 mm) was sandwiched between two glass substrates in water and stored in the water for different times. Then the adhered plates were clamped to the universal testing machine and pulled at a crosshead speed of 10 mm min^{-1}. The adhesion strength was calculated by the measured maximum load divided by the bonded area. Each sample was tested three times in parallel.

Supporting Information
Supporting Information is available from the Wiley Online Library or from the author.

Conflict of Interest
The authors declare no conflict of interest.

References

[1]   a) H. L. Fan, J. P. Gong, *Macromolecules* **2020**, *53*, 2769; b) J. Sun, J. Su, C. Ma, R. Göstl, A. Herrmann, K. Liu, H. Zhang, *Adv. Mater.* **2020**, *32*, 1906360; c) Y. Chen, J. Meng, Z. Gu, X. Wan, L. Jiang, S. Wang, *Adv. Funct. Mater.* **2019**, *30*, 1905287.

[2]   a) M. Dompé, F. J. Cedano-Serrano, O. Heckert, N. van den Heuvel, J. van der Gucht, Y. Tran, D. Hourdet, C. Creton, M. Kamperman, *Adv. Mater.* **2019**, *31*, 1808179; b) Q. Zhao, D. W. Lee, B. K. Ahn, S. Seo, Y. Kaufman, J. N. Israelachvili, J. H. Waite, *Nat. Mater.* **2016**, *15*, 407; c) K. Kim, M. Shin, M.-Y. Koh, J. H. Ryu, M. S. Lee, S. Hong,

H. Lee, *Adv. Funct. Mater.* **2015**, *25*, 2402; d) H. Shao, R. J. Stewart, *Adv. Mater.* **2010**, *22*, 729.

[3]   a) J. Li, A. D. Celiz, J. Yang, Q. Yang, I. Wamala, W. Whyte, B. R. Seo, N. V. Vasilyev, J. J. Vlassak, Z. Suo, D. J. Mooney, *Science* **2017**, *357*, 378; b) H. Yuk, C. E. Varela, C. S. Nabzdyk, X. Mao, R. F. Padera, E. T. Roche, X. Zhao, *Nature* **2019**, *575*, 169; c) X. Li, Y. Deng, J. Lai, G. Zhao, S. Dong, *J. Am. Chem. Soc.* **2020**, *142*, 5371.

[4]   a) C. Cui, C. Fan, Y. Wu, M. Xiao, T. Wu, D. Zhang, X. Chen, B. Liu, Z. Xu, B. Qu, W. Liu, *Adv. Mater.* **2019**, *31*, 1905761; b) Z. Wang, L. Guo, H. Xiao, H. Cong, S. Wang, *Mater. Horiz.* **2020**, *7*, 282; c) A. Beharaj, E. Z. McCaslin, W. A. Blessing, M. W. Grinstaff, *Nat. Commun.* **2019**, *10*, 5478.

[5]   a) A. Cholewinski, F. Yang, B. Zhao, *Mater. Horiz.* **2019**, *6*, 285; b) F. Pan, S. Ye, R. Wang, W. She, J. Liu, Z. Sun, W. Zhang, *Mater. Horiz.* **2020**, *7*, 2063.

[6]   a) S. K. Clancy, A. Sodano, D. J. Cunningham, S. S. Huang, P. J. Zalicki, S. Shin, B. K. Ahn, *Biomacromolecules* **2016**, *17*, 1869; b) Y. Zhao, Y. Wu, L. Wang, M. Zhang, X. Chen, M. Liu, J. Fan, J. Liu, F. Zhou, Z. Wang, *Nat. Commun.* **2017**, *8*, 2218.

[7]   J. K. Park, J. D. Eisenhaure, S. Kim, *Adv. Mater. Interfaces* **2019**, *6*, 1801542.

[8]   a) L. Han, M. Wang, L. O. Prieto-López, X. Deng, J. Cui, *Adv. Funct. Mater.* **2020**, *30*, 1907064; b) X. Fan, W. Zhou, Y. Chen, L. Yan, Y. Fang, H. Liu, *ACS Appl. Mater. Interfaces* **2020**, *12*, 32031; c) C. Cui, T. Wu, X. Chen, Y. Liu, Y. Li, Z. Xu, C. Fan, W. Liu, *Adv. Funct. Mater.* **2020**, 2005689; d) H. Qiao, P. Qi, X. Zhang, L. Wang, Y. Tan, Z. Luan, Y. Xia, Y. Li, K. Sui, *ACS Appl. Mater. Interfaces* **2019**, *11*, 7755; e) X. Liu, Q. Zhang, L. Duan, G. Gao, *ACS Appl. Mater. Interfaces* **2019**, *11*, 6644; f) H. L. Fan, J. H. Wang, Z. Tao, J. C. Huang, P. Rao, T. Kurokawa, J. P. Gong, *Nat. Commun.* **2019**, *10*, 5127; g) P. Rao, T. L. Sun, L. Chen, R. Takahashi, G. Shinohara, H. Guo, D. R. King, T. Kurokawa, J. P. Gong, *Adv. Mater.* **2018**, *30*, 1801884.

[9]   a) H. Yi, S. H. Lee, M. Seong, M. K. Kwak, H. E. Jeong, *J. Mater. Chem. B* **2018**, *6*,

8064; b) S. Baik, J. Kim, H. J. Lee, T. H. Lee, C. Pang, *Advanced Science* **2018**, *5*, 1800100; c) S. H. Lee, H. W. Song, B. S. Kang, M. K. Kwak, *ACS Appl. Mater. Interfaces* **2019**, *11*, 47571.

[10]   L. C. Bradley, N. D. Bade, L. M. Mariani, K. T. Turner, D. Lee, K. J. Stebe, *ACS Appl. Mater. Interfaces* **2017**, *9*, 27409.

[11]   C. Creton, M. Ciccotti, *Rep. Prog. Phys.* **2016**, *79*, 046601.

[12]   a) X. H. Zhao, *Soft Matter* **2014**, *10*, 672; b) T. L. Sun, T. Kurokawa, S. Kuroda, A. B. Ihsan, T. Akasaki, K. Sato, M. A. Haque, T. Nakajima, J. P. Gong, *Nat. Mater.* **2013**, *12*, 932.

[13]   J. H. Waite, *J. Exp. Biol.* **2017**, *220*, 517.

[14]   J. N. Israelachvili, *London: Elsevier. 3rd edition* **2010**.

[15]   A. H. Hofman, I. A. van Hees, J. Yang, M. Kamperman, *Adv. Mater.* **2018**, *30*, 1704640.

[16]   K. Kamino, in *Biological Adhesives* (Eds.: A. M. Smith, J. A. Callow), Springer Berlin Heidelberg, Berlin, Heidelberg, **2006**, pp. 145.

[17]   a) M. Rocha, P. Antas, L. F. C. Castro, A. Campos, V. Vasconcelos, F. Pereira, I. Cunha, *Mar. Biotechnol.* **2018**, *21*, 38; b) Z. Wang, D. H. Leary, J. Liu, R. E. Settlage, K. P. Fears, S. H. North, A. Mostaghim, T. Essock-Burns, S. E. Haynes, K. J. Wahl, C. M. Spillmann, *BMC Genomics* **2015**, *16*, 859.

[18]   Y. Urushida, M. Nakano, S. Matsuda, N. Inoue, S. Kanai, N. Kitamura, T. Nishino, K. Kamino, *The FEBS Journal* **2007**, *274*, 4336.

[19]   a) C. D. Ma, C. Wang, C. Acevedo-Vélez, S. H. Gellman, N. L. Abbott, *Nature* **2015**, *517*, 347; b) C. Liang, J. Strickland, Z. Ye, W. Wu, B. Hu, D. Rittschof, *Frontiers in Marine Science* **2019**, *6*, 565.

[20]   a) J. A. Hunt, C. A. Fierke, *J. Biol. Chem.*, **1997**, 272, 20364; b) Y. Akdogan, W. Wei, K.-Y. Huang, Y. Kageyama, E. W. Danner, D. R. Miller, N. R. Martinez Rodriguez, J. H. Waite, S. Han, *Angew. Chem. Int. Ed.*, **2014**, 53, 11253; c) G. P. Maier, M. V. Rapp,

J. H. Waite, J. N. Israelachvili, A. Butler, *Science*, **2015**, 349, 628.

[21]   H. Guo, T. Nakajima, D. Hourdet, A. Marcellan, C. Creton, W. Hong, T. Kurokawa, J. P. Gong, *Adv. Mater.* **2019**, *31*, 1900702.

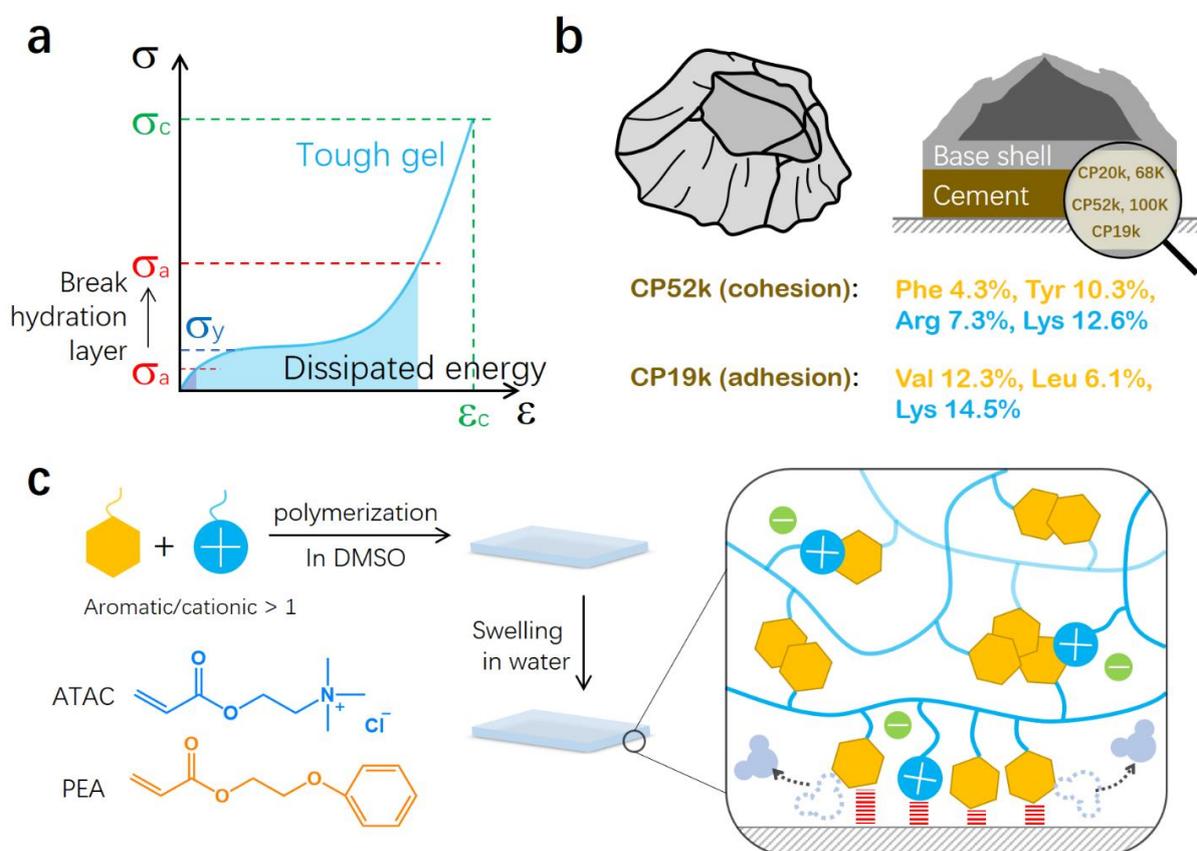[22]   T. L. Sun, F. Luo, T. Kurokawa, S. N. Karobi, T. Nakajima, J. P. Gong, *Soft Matter* **2015**, *11*, 9355.

Figure 1. Schematic design strategy for hydrogel adhesives with robust, long-lasting, and repeatable underwater adhesion. a) An illustration of the general mechanical principle for a strong adhesive. The blue curve represents the bulk tensile stress-strain curve of soft, but tough, material with yielding stress (σ_y) fracture stress (σ_c) and fracture strain (ε_c). The red dashed lines represent the debonding stress (σ_a) of the adhesive interface. A strong but reversible adhesive requires a large σ_c and ε_c in bulk and a large σ_a at the interface with $\sigma_y \ll \sigma_a < \sigma_c$, allowing for significant energy dissipation without cohesive failure. For hydrogel adhesives, while large σ_c and ε_c can be obtained by dynamic bonds, achieving a large σ_a in water is challenging due to the hydration of interfaces underwater. b) Schematic of a barnacle, its cross-section, and the cationic (Arg and Lys) and hydrophobic (Phe, Tyr, Val, and Leu) amino acid contents in the two CPs: CP52k for cohesion in the bulk and CP19k for adhesion at the interface. c) Schematic of the molecular mechanism to fabricate underwater adhesive

hydrogels. Cationic 2-(acryloyloxy)ethyl trimethylammonium chloride (ATAC) and aromatic 2-phenoxyethyl acrylate (PEA) monomers were adopted to mimic the cationic and hydrophobic amino acids in barnacle CPs, respectively. π-π and cation-π interactions provide dynamic bonds in the bulk hydrogel to show high toughness, while they cause dehydration at the interface to promote electric and hydrophobic interactions, which results in a large σ_a.
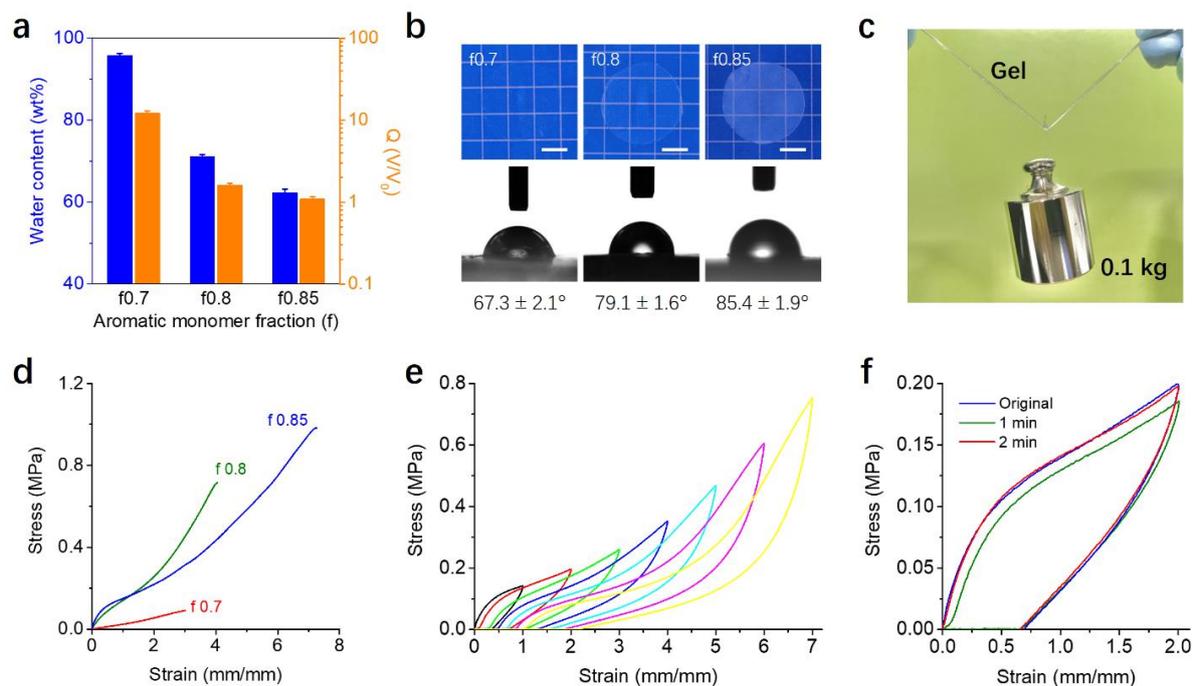

Figure 2. Mechanical properties of poly(ATAC-co-PEA) hydrogels with different aromatic monomer fractions (f). a) Water content and swelling ratio of hydrogels. b) Digital photos and contact angle of hydrogels to water. c) A digital photo showing that a string of tough hydrogel (f = 0.85) can hold a load. d) Tensile stress-strain curves of hydrogels with different f values. e) Representative cyclic tensile loading-unloading curves with a gradual strain increase for the f = 0.85 hydrogel. f) Hysteresis and self-recovery of the f = 0.85 hydrogel measured by cyclic tensile tests. The initial strain rate of tensile tests was 0.14 s^{-1}. The numbers in (b) and (d) are the f values.
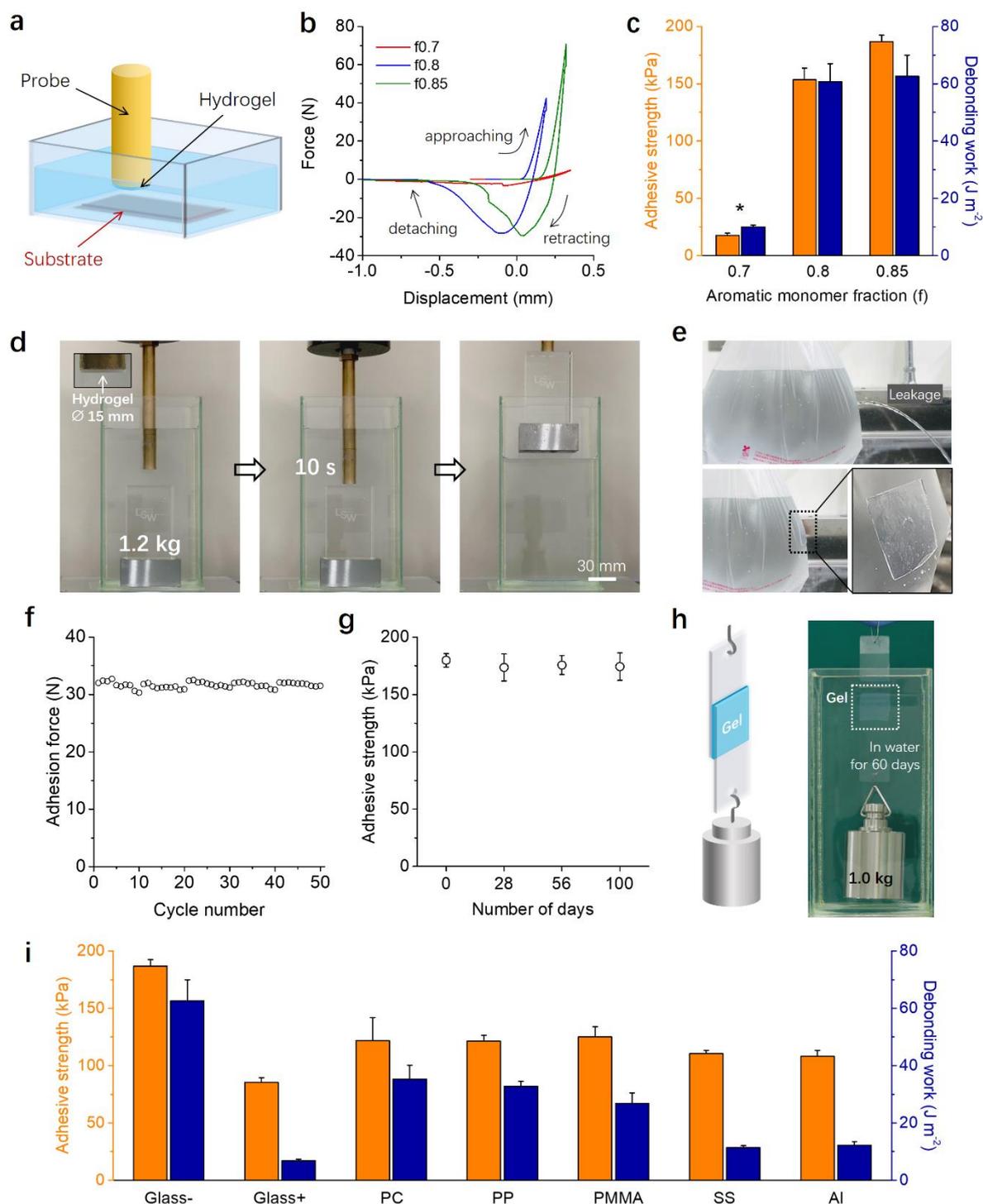
Figure 3. Underwater adhesion of poly(ATAC-co-PEA) hydrogels. a) Schematic diagram of the tack test to measure the underwater adhesion. b) Force-displacement curves of poly(ATAC-co-PEA) hydrogels with different aromatic monomer fractions adhered to a negatively charged glass substrate in water. c) Adhesion values of poly(ATAC-co-PEA) hydrogels adhered to a negatively charged glass substrate in water. The result marked by an asterisk indicates that the failure occurred in the bulk of hydrogel, not at the interface. d) Photographs of the f = 0.85 gel adhered to a 1.2 kg block in water and then lifted out of the water to the air. e) Photographs showing that the f = 0.85 gel could mend the hole in a plastic bag to immediately stop water leakage. f) Repeated adhesion of the f = 0.85 gel (diameter 15 mm) to a negatively charged glass substrate in water based on the tack test. The sample was

placed at rest underwater for 3 min between two successive tests, and a new glass substrate was used every ten tests. g) Long-lasting adhesion values of the f = 0.85 gel after immersing the gel-joined glass plates in water for a different number of days based on the lap-shear test. h) Photograph showing the f = 0.85 gel adhered firmly to glass after 60 days. i) Adhesion values of the f = 0.85 hydrogels to a variety of substrates with different types of surface charges and hydrophobicity in water. PC: polycarbonate, PP: polypropylene, PMMA: poly(methyl methacrylate), SS: stainless steel, Al: aluminum. The error bars indicate the standard deviation (N = 5).
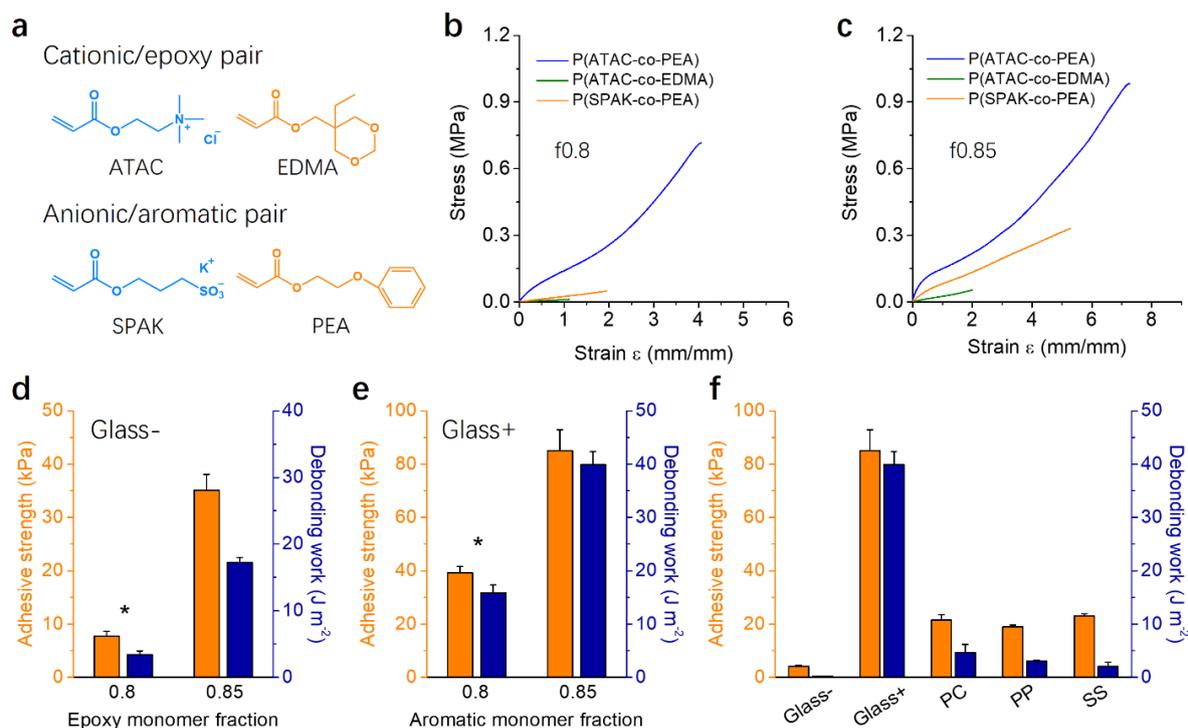
Figure 4. a) Monomer structures of control hydrogels. b, c) Tensile stress-strain curves of hydrogels with a hydrophobic monomer fraction of f = 0.8 (b) and f = 0.85 (c). d) Adhesion values of poly(ATAC-co-EDMA) hydrogels to a negatively charged glass substrate in water. e) Adhesion values of poly(SPAK-co-PEA) hydrogels to a positively charged glass substrate in water. f) Adhesion values of poly(SPAK-co-PEA) hydrogels (f = 0.85) to a variety of substrates with different types of surface charges and hydrophobicity in water. The results marked by an asterisk indicate that the fracture occurred in the bulk of hydrogel, and not at the interface. The error bars indicate the standard deviation (N = 5).
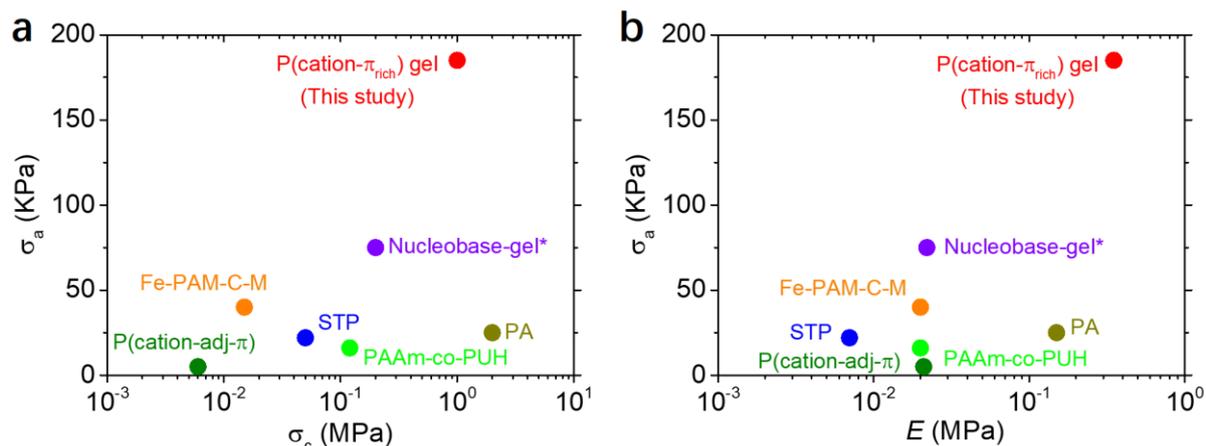
Figure 5. Comparison of the underwater adhesion strength and cohesion strength of various hydrogels reported in literatures and the poly(ATAC-co-PEA) (f = 0.85) hydrogels developed in this work, shortly named as P(cation-π_{rich}) gel. The best adhesive strength in water is plotted against the tensile strength (a) and elastic modulus (b) for various underwater adhesive hydrogels reported in the literature, including nucleobase-gel (*adhesion is introduced by the organic solvent exchange process),[8e] Fe-PAM-C-M gel,[8a] STP gel,[8d] P(cation-adj-π) gel,[8f] PA gel,[8g] and PAAm-co-PUH gel.[8b] To conduct a rational comparison, only hydrogels showing instant in-situ underwater adhesiveness are compared. Note that the adhesion strength might differ because of the differences in measuring conditions.

The hydrogel consisting of a crosslinked copolymer of cationic and aromatic monomers shows instant and robust underwater adhesion to diverse substrates. This is because the aromatic groups provide hydrophobic adhesion and enhance the electrostatic adhesion of their neighboring cationic groups.

H. L. Fan, J. H. Wang, J. P. Gong*

Barnacle Cement Proteins Inspired Tough Hydrogels with Robust, Long-lasting, and Repeatable Underwater Adhesion

ToC figure
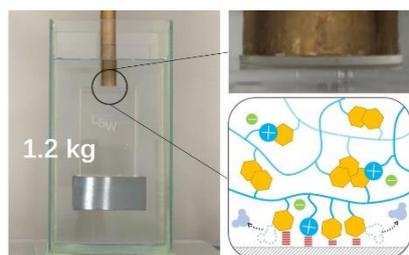
Supporting Information

Barnacle Cement Proteins Inspired Tough Hydrogels with Robust, Long-lasting, and Repeatable Underwater Adhesion

Hailong Fan,[1] Jiahui Wang,[2] and Jian Ping Gong[1,3,4]*

[1]Institute for Chemical Reaction Design and Discovery (WPI-ICReDD), Hokkaido University, N21W10, Kita-ku, Sapporo 001-0021, Japan

[2]Graduate School of Life Science, Hokkaido University, N21W11, Kita-ku, Sapporo 001-0021, Japan

[3]Faculty of Advanced Life Science, Hokkaido University, N21W11, Kita-ku, Sapporo 001-0021, Japan

[4]Global Station for Soft Matter GI-CoRE, Hokkaido University, N21W11, Kita-ku, Sapporo 001-0021, Japan

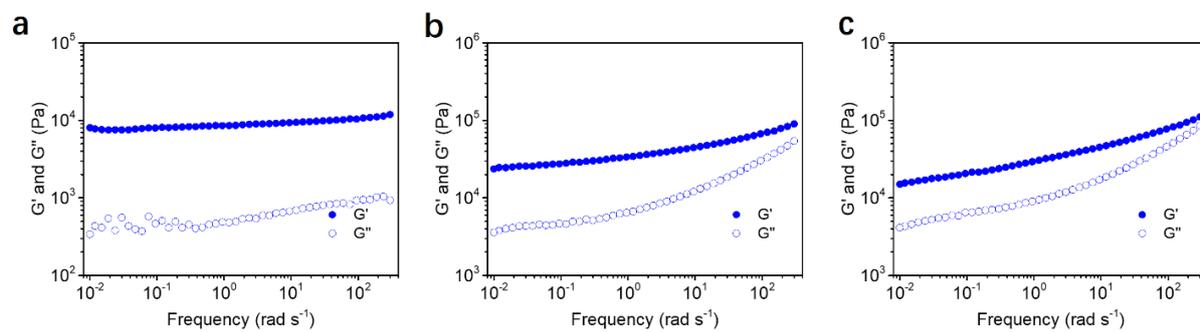*Correspondence to: gong@sci.hokudai.ac.jp

Supplementary Figures

Figure S1. The storage modulus G' and the loss modulus G'' as a function of angular frequency of poly(ATAC-co-PEA) hydrogels with different PEA molar fraction f. (a) f = 0.7, (b) f = 0.8, (c) f = 0.85.

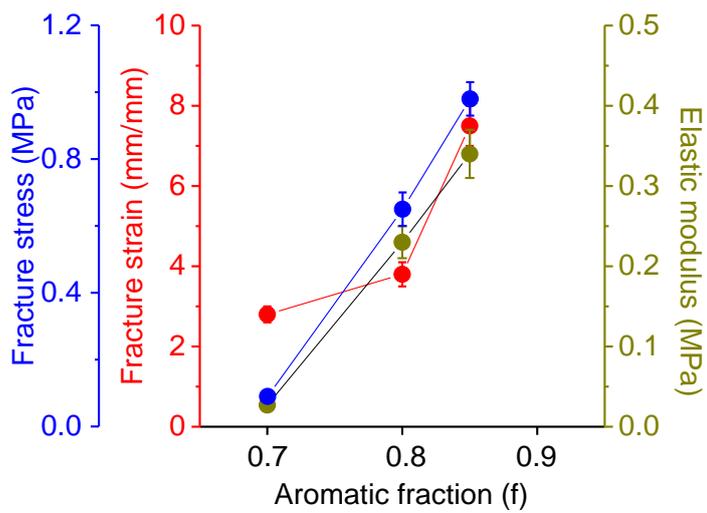Figure S2. The fracture stress, fracture strain, and elastic modulus of poly(ATAC-co-PEA) hydrogels with different f obtained from stress–strain curves in Figure 2d of the main text.
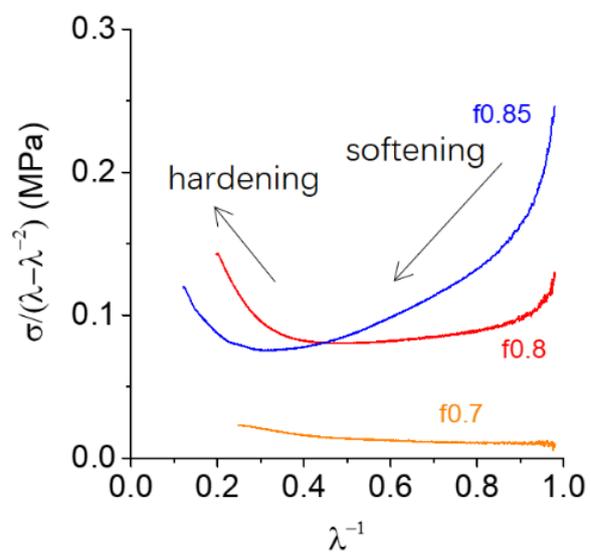
Figure S3. Mooney−Rivlin curves of poly(ATAC-co-PEA) hydrogels with different PEA fraction f. σ is stress and λ is the extension ratio, which is related to the strain ε as λ = ε +1.
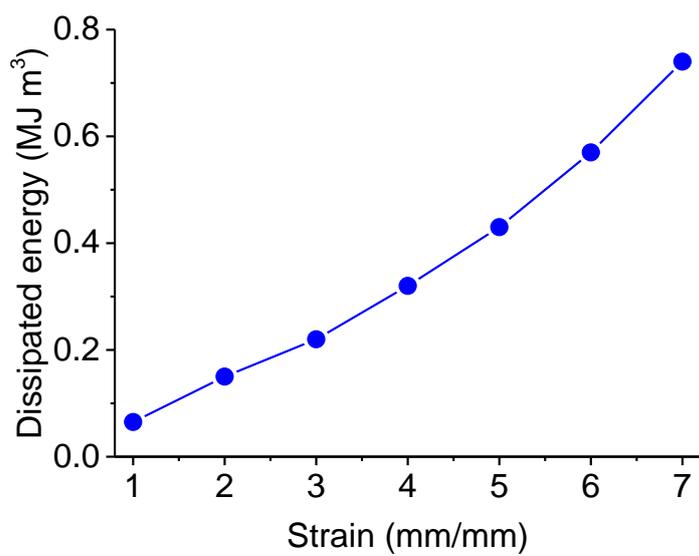
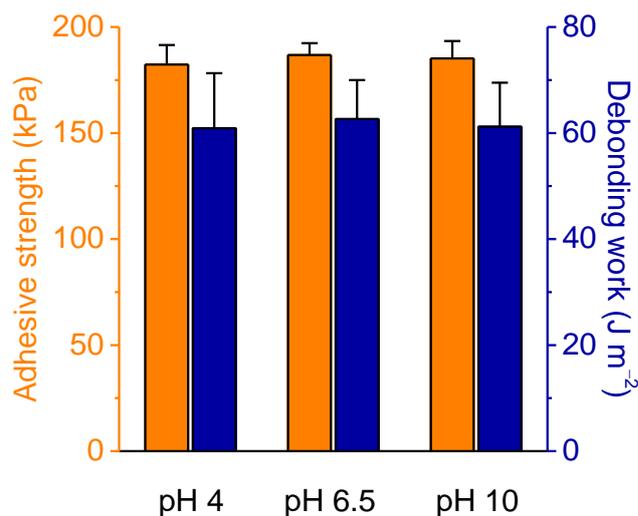Figure S4. The dissipated energy of poly(ATAC-co-PEA) hydrogel (f = 0.85) under different

strain.

Figure S5. Adhesion values of poly(ATAC-co-PEA) hydrogels (f = 0.85) in water of different pH values. Error bars indicate standard deviation (N = 5). The tack tests were performed at a normal pressure equivalent to the elastic modulus E of the gels. All the tests were performed on a glass substrate. The acidic and basic solutions were prepared by dissolving HCl and NaOH in water, respectively. The ionic strength of pH 4 and pH 10 solutions was ~10^{-4} M. The swelling ratio and mechanical properties of the hydrogels in pH 4 and pH 10 solutions were the same as that in water (pH 6.5).
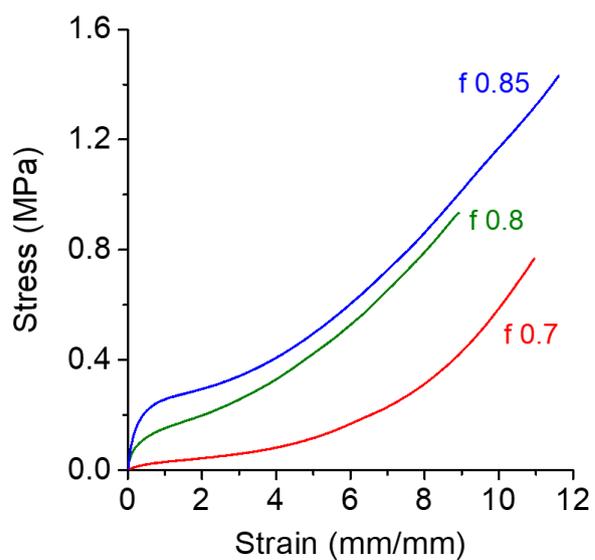
Figure S6. Tensile stress-strain curves of poly(ATAC-co-PEA) hydrogels with different PEA monomer fraction f. All samples were reached equilibrium in 0.7 M NaCl.
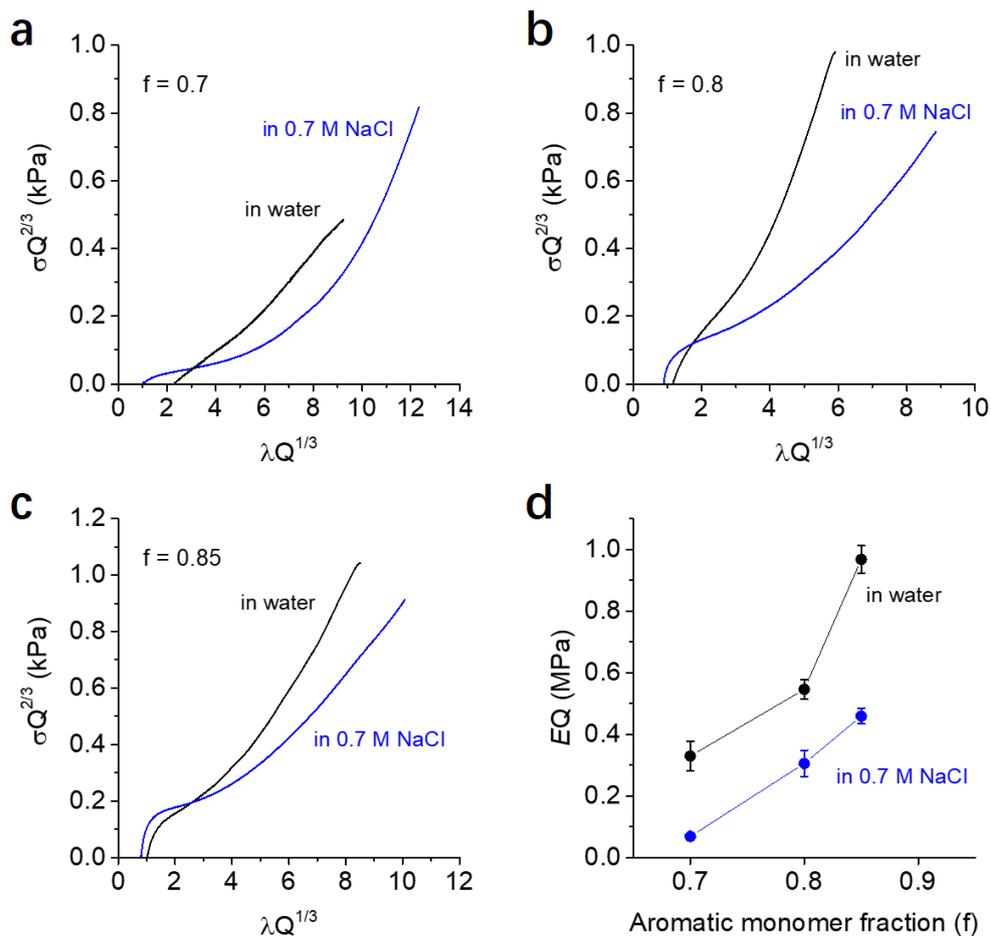
Figure S7. (a-c) Normalized tensile stress-strain curves of poly(ATAC-co-PEA) hydrogels in water and in 0.7 M NaCl solution. (a) f= 0.7. (b) f=0.8. (c) f=0.85. σ is stress of hydrogels. λ is the extension ratio, which is related to the strain ε as $\lambda = \varepsilon +1$. Q is the volume swelling ratio of hydrogels in relative to their as-prepared state. (d) Normalized elastic modulus of hydrogels in water and in 0.7 M NaCl solution.
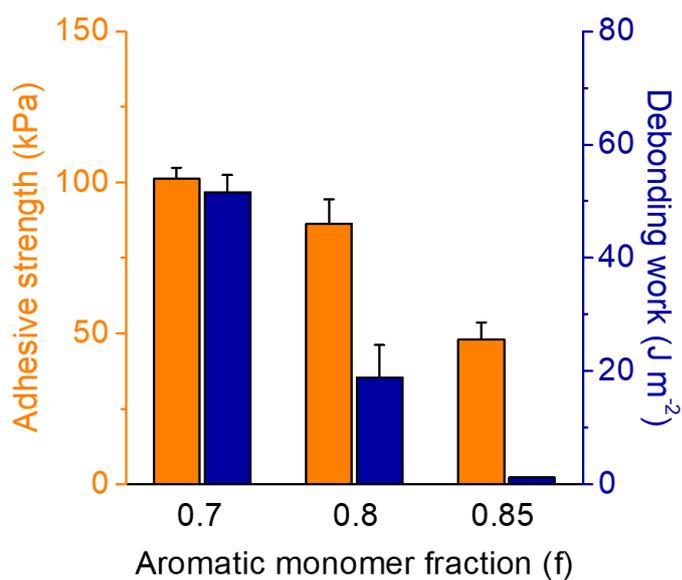
Figure S8. Adhesion values of poly(ATAC-co-PEA) hydrogels with different PEA fraction f in 0.7 M NaCl solution. All samples were reached equilibrium in 0.7 M NaCl. Error bars indicate standard deviation (N = 5). All the tack tests were performed on a glass substrate. The pressures of tack test were equivalent to 100%E, 50%E, 30%E of f = 0.7, f = 0.8, and f = 0.85 gels, respectively, where E is the elastic modulus of the corresponding hydrogels.
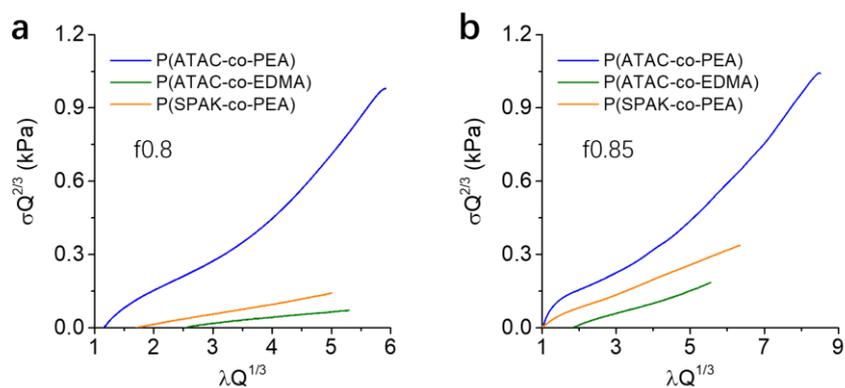
Figure S9. Normalized tensile stress-extension ratio curves of hydrogels with different monomer pairs in water. (a) f= 0.8. (b) f=0.85. σ is stress of hydrogels. λ is the extension ratio, which is related to the strain ε as $\lambda = \varepsilon +1$. Q is the volume swelling ratio of hydrogels in relative to their as-prepared states.

Supplementary Tables

Supplementary Table 1. Formulation of samples synthesized in this study and swelling behavior in water.

Samples	hydrophobic monomer molar fraction (f)	Water content C_w(wt%)	Swelling ratio Q*
P(ATAC-*co*-PEA)	0.7	95.8±0.5	12.2±0.7
	0.8	71.0±0.5	1.6±0.08
	0.85	62.3±0.8	1.1±0.06
P(ATAC-*co*-EDMA)	0.8	98.4±0.1	15.6±0.9
	0.85	94.5±0.4	6.3±0.4
P(SPAK-*co*-PEA)	0.8	94.2±0.14	4.9±0.2
	0.85	79.7±0.7	1.1±0.05

*: $Q=V/V_0$, where V and V_0 are volumes of the gels in water and in as-prepared state in DMSO, respectively.

Supplementary Table 2. Mechanical properties, volume swelling ratio, and underwater adhesion of P(ATAC-co-PEA) hydrogels in water and in 0.7 M NaCl solution.

In water					
Gel	Stress (MPa)	Strain (mm/mm)	Elastic modulus (MPa)	Swelling ratio, Q^*	Underwater adhesion (kPa)
f 0.7	0.09±0.01	2.8±0.2	0.027±0.002	12.2±0.7	17.5±2.1
f 0.8	0.65±0.05	3.8±0.3	0.23±0.02	1.6±0.08	153.4±10.3
f 0.85	0.98±0.05	7.5±0.5	0.34±0.03	1.1±0.06	186.7±5.6
In 0.7 M NaCl solution					
Gel	Stress (MPa)	Strain (mm/mm)	Elastic modulus (MPa)	Swelling ratio, Q^*	Underwater adhesion (kPa)
f 0.7	0.82±0.06	11.2±0.9	0.063±0.004	1.1±0.1	101.2±3.8
f 0.8	0.95±0.12	9.1±0.6	0.43±0.06	0.71±0.08	86.4±8.2
f 0.85	1.3±0.1	11.3±0.8	0.91±0.05	0.51±0.09	48.1±5.6

*: $Q=V/V_0$, where V and V_0 are volumes of the gels in water or 0.7 M NaCl solution and in as-prepared state in DMSO, respectively.

Supplementary Table 3. Comparison of fast bonding adhesives in water.

Adhesives type	Component*	Adhesion strength	Bonding time	Reversibility	Stability	Ref.
Glue (Coacervate)	PVA + Tannic acid	40~70 kPa	30 s	10 cycles no decrease	168 h	[1]
Glue (liquid polymer)	Liquid PDMS + PTFE particles	2~35 kPa	Instant	No data	No data	[2]
Glue (liquid polymer)	PPGBC	240 kPa	5 s	No data	No data	[3]
Glue (liquid polymer)	hyperbranched polymer with catechol	10~14 kPa	10 s	5 cycles decrease 50%	12 h decrease 40%	[4]
Glue (liquid polymer)	Anthracenyl-PEI	50~600 kPa**	2 s ~ 2.5 min	yes	No data	[5]
Tape (rubber)	Poly(epoxy)	0.15~1.8 MPa	Minutes***	4 cycles decrease 95%	No data	[6]
Tape (polymer film)	Catechol-based polymer	50~150 kPa	Instant	No data	No data	[7]
Tape (hydrogel)	PAAm-SDS-Fe	10~40 kPa	120 s	50 cycles no decrease	15 days decrease 25%	[8]
Tape (hydrogel)	PAAm + Tannic acid + sodium alginate	10~20 kPa	Instant	No data	No data	[9]
Tape (hydrogel)	Poly(AAm-co-UH)	16 kPa	2 min	5 cycles decrease 20%	2.5 hours decrease 18%	[10]
Tape (hydrogel)	Poly(ATAC-co-PEA)	150~180 kPa	10 s	50 cycles no decrease	8 weeks no decrease	This work

* PVA: poly(vinyl alcohol), PDMS: polydimethylsiloxane, PTFE: polytetrafluoroethylene, PPGBC: Poly (propylene-co-glycidyl butyrate carbonate), PEI: polyethylenimine, PAAm: polyacrylamide, SDS: sodium dodecyl sulfate, UH: urushiol. **Adhesive strength depends on the irradiation time. *** depends on the heating temperature. Note that the adhesion strength may be different because of the difference in measuring conditions.

References:

1. Lee, D.; Hwang, H.; Kim, J.-S.; Park, J.; Youn, D.; Kim, D.; Hahn, J.; Seo, M.; Lee, H. VATA: A Poly(vinyl alcohol)- and Tannic Acid-Based Nontoxic Underwater Adhesive. *ACS Appl. Mater. Interfaces* **2020,** 12, 20933-20941.

2. Chipara, A. C.; Tsafack, T.; Owuor, P. S.; Yeon, J.; Junkermeier, C. E.; van Duin, A. C. T.; Bhowmick, S.; Asif, S. A. S.; Radhakrishnan, S.; Park, J. H.; Brunetto, G.; Kaipparettu, B. A.; Galvão, D. S.; Chipara, M.; Lou, J.; Tsang, H. H.; Dubey, M.; Vajtai, R.; Tiwary, C. S.; Ajayan, P. M. Underwater adhesive using solid–liquid polymer mixes. *Mater. Today Chem.* **2018,** 9, 149-157.

3. Beharaj, A.; McCaslin, E. Z.; Blessing, W. A.; Grinstaff, M. W. Sustainable polycarbonate adhesives for dry and aqueous conditions with thermoresponsive properties. *Nat. Commun.* **2019,** 10, 5478.

4. Cui, C.; Fan, C.; Wu, Y.; Xiao, M.; Wu, T.; Zhang, D.; Chen, X.; Liu, B.; Xu, Z.; Qu, B.; Liu, W. Water-Triggered Hyperbranched Polymer Universal Adhesives: From Strong Underwater Adhesion to Rapid Sealing Hemostasis. *Adv. Mater.* **2019,** 31, 1905761.

5. Wang, Z.; Guo, L.; Xiao, H.; Cong, H.; Wang, S. A reversible underwater glue based on photo- and thermo-responsive dynamic covalent bonds. *Mater. Horiz.* **2020,** 7, 282-288.

6. Park, J. K.; Eisenhaure, J. D.; Kim, S. Reversible Underwater Dry Adhesion of a Shape Memory Polymer. *Adv. Mater. Interfaces* **2019,** 6, 1801542.

7. Clancy, S. K.; Sodano, A.; Cunningham, D. J.; Huang, S. S.; Zalicki, P. J.; Shin, S.; Ahn, B. K. Marine Bioinspired Underwater Contact Adhesion. *Biomacromolecules* **2016,** 17, 1869-1874.

8. Han, L.; Wang, M.; Prieto-López, L. O.; Deng, X.; Cui, J. Self-Hydrophobization in a Dynamic Hydrogel for Creating Nonspecific Repeatable Underwater Adhesion. *Adv. Funct. Mater.* **2020,** 30, 1907064.

9. Qiao, H.; Qi, P.; Zhang, X.; Wang, L.; Tan, Y.; Luan, Z.; Xia, Y.; Li, Y.; Sui, K. Multiple Weak

H-Bonds Lead to Highly Sensitive, Stretchable, Self-Adhesive, and Self-Healing Ionic Sensors. *ACS Appl. Mater. Interfaces* **2019,** 11, 7755-7763.

10. Fan, X.; Zhou, W.; Chen, Y.; Yan, L.; Fang, Y.; Liu, H. An Antifreezing/Antiheating Hydrogel Containing Catechol Derivative Urushiol for Strong Wet Adhesion to Various Substrates. *ACS Appl. Mater. Interfaces* **2020,** 12, 32031-32040.